

REFINEMENT OF MICROSTRUCTURE OF SEVERAL γ -TiAl ALLOYS BY MASSIVE TRANSFORMATION AND EFFECT OF REFINEMENT ON COMPRESSION PROPERTIES

JUŘICA Jan, SKOTNICOVÁ Kateřina, PETLÁK Daniel

VSB-Technical University of Ostrava, FMMI, RMTVC, Ostrava, Czech Republic, EU, jan.jurica@vsb.cz

Abstract

The possibilities of microstructure refinement of several γ -TiAl alloys by the massive transformation and the effect of refinement on compression properties are discussed in this paper. Two alloys were prepared by plasma arc melting using the water-cooled copper crystallizer and two other alloys were prepared by vacuum induction melting. All alloys were subjected to subsequent two-step heat treatment, which consisted of the dissolving annealing followed by the ageing. This procedure resulted in the considerable reduction of the mean grain size from 200-340 μm to 70-35 μm . The microstructure refinement led to the increase of values of the plastic deformation in compression, namely from 9-17 % to 25-30 %. This effect denotes the substantial decrease of brittleness of these intermetallic alloys as a result of the used heat treatment.

Keywords: γ -TiAl alloys, plasma arc melting, vacuum induction melting, massive transformation, mechanical properties

1. INTRODUCTION

γ -TiAl based alloys are very perspective materials thanks to their outstanding properties, such as high specific strength, low density, high modulus of elasticity, good oxidation resistance and resistance to creep. In many applications in aircraft, power and automotive industries they might replace the currently used materials, such as nickel based superalloys, which are characterized by higher density. One of the main reasons why it happens only in very limited extent is their brittleness and complicated production of components [1-3]. Brittleness is characterized by low values of elongation at room temperature, which are usually less than 1%. This value is generally considered as the minimum acceptable level for structural parts in the above mentioned sectors [2, 3]. A suitable combination of strength, creep resistance, toughness and ductility have the recently developed alloys γ -TiAl of the third and fourth generation, containing relatively high amounts of refractory metals (5-10 at.% Nb, Ta) [2-6]. These alloys, however, are in the cast state characterized by a coarse-grained microstructure, which has a negative effect on mechanical properties. For this reason it is necessary to refine the final microstructure. Reducing the grain size improves significantly room-temperature ductility without degradation of creep resistance. There are main two approaches to refining of the coarse grained structure of γ -TiAl based alloys: (i) affecting of solidification path by alloying with minor addition of boron, and (ii) formation of highly faulted massive γ_m through diffusionless transformation initiated by cooling at the required rate from single α phase field [4-6]. Progress of massive transformation depends on many factors, but primarily upon the chemical composition of the alloy and on the cooling rate [4, 5]. Huang et al. show that massive transformation is also very sensitive to the oxygen content, the higher content of which prevents the massive transformation to the γ_m phase [7]. The aim of this article is to characterize the possibilities of microstructure refinement by massive transformation in four different alloys, prepared by two different processes. Other goals consisted in assessment of the impact of alloying elements on the course of massive transformation, and in determination of the effect of refining on compression mechanical properties.

2. EXPERIMENT

Two alloys with a nominal composition Ti-47Al-8Nb and Ti-47Al-8Nb-0.3Y (at.%) were prepared in the plasma furnace with a horizontal water-cooled copper mold. Pieces of pure elements (99.9 %) and master alloy Nb-

60Al (at.%) were used as a charge, the preparation of which and properties presented in another article [8]. Melting was conducted with crystallizer feed rate of 2 cm/min, in a flowing Ar atmosphere and the maximum current density of 700 A. The products were oval cross-section ingots weighing 600 g. Two another γ -TiAl-based alloys with nominal composition Ti-47Al-8Ta and Ti-47Al-8Ta-0.3Y (at.%) were prepared by induction melting in graphite crucible and centrifugal casting into graphite mould. The conditions and materials used during the melting were presented in the article [9]. Samples with the length of 50 mm, which were subsequently used for mechanical tests and for heat treatment for the purpose of massive transformation, were prepared by EDM cut-outs taken from the central parts of all ingots.

The samples were analyzed using optical microscopy (OM) and electron scanning microscopy in the mode of back-scattered electrons (BSE). Chemical composition was determined by energy dispersive analysis (EDS) on both ends of the samples taken by spark erosion machining. The program analySIS auto using images obtained by optical microscopy was used for determination of contents of individual phases and grain size. Oxygen and carbon contents were determined by thermo-evolution method on instruments ELTRA ONH-2000 and ELTRA CS-2000. **Table 1** presents a list of all the samples that were subjected to heat treatment in order to achieve convoluted microstructure, including the chemical composition determined by EDS and detected oxygen and carbon contents in the samples before the heat treatment.

Table 1 Chemical composition of alloys before the heat treatment

| Sample | Chemical composition (at.%) | | | | | Oxygen content (wt.ppm) | Carbon content (wt.ppm) |
|--------------|-----------------------------|------|------|-------|------|-------------------------|-------------------------|
| | Ti | Nb | Ta | Al | Y | | |
| 8Nb-plasma | 44.83 | 7.37 | - | 47.80 | - | 351 ± 69 | 89 ± 09 |
| 8Nb-Y-plasma | 44.25 | 8.15 | - | 47.45 | 0.25 | 586 ± 42 | 92 ± 13 |
| 8Ta-Scast | 42.06 | - | 8.28 | 49.66 | - | 334 ± 50 | 463 ± 37 |
| 8Ta-Y-Scast | 43.40 | - | 8.59 | 47.59 | 0.41 | 460 ± 82 | 1023 ± 42 |

The conditions of the two-step heat treatment consist of solution annealing in a muffle furnace in air, with quenching in oil or with cooling by fan, followed by annealing in the sintering furnace XERION XVAC in Ar (5N) atmosphere at lower temperatures, are presented in **Table 2**.

Table 2 Overview of thermal processing and measurement results of oxygen content

| Sample | Solution annealing | Cooling | Ageing | Oxygen content (wt. ppm) |
|--------------|--------------------|---------|-----------------------|--------------------------|
| 8Nb-plasma | 1370 °C / 10 min. | Oil | 1280 °C / 2 h / FC | 621 ± 24 |
| 8Nb-Y-plasma | 1370 °C / 10 min. | Oil | 1280 °C / 2 h / FC | 628 ± 13 |
| 8Ta-Scast | 1360 °C / 10 min. | Air | 1260 °C / 30 min / FC | 447 ± 23 |
| 8Ta-Y-Scast | 1360 °C / 10 min. | Air | 1260 °C / 30 min / FC | 541 ± 36 |

This table presents also the detected oxygen contents after heat treatment. The samples with dimensions 4 x 4 x 8 mm were used for mechanical compression tests at ambient temperature. The tests were conducted on the universal testing equipment Walter Bai TMS LFV 100 kN at room temperature with the initial crosspiece velocity of 0.2 mm/min. The resulting values of mechanical properties were taken from the diagrams showing the relationship between strain and stress. The amount of deformation was determined by the ratio between the change of the length of the sample during the compression test and its initial length. Proof stress $R_{p0.2}$ was determined from the diagrams with use of a line parallel to the linear part of the diagram at the distance, which corresponds to plastic deformation of 0.2 %. Tensile strength R_m was determined as the highest value of the normal stress, the excess of which caused a failure of material cohesion. Plastic deformation to ultimate

strength (ϵ_{Rm}) was determined as the difference between the value of deformation from the point of diversion of the curve of dependence of deformation on stress from the linear shape and the value of deformation after reaching the ultimate strength R_m .

3. RESULTS AND DISCUSSION

3.1. Microstructure of alloys in as-cast state

Typical microstructure of the prepared alloys, which is typically formed by coarse grains (up to 500 μm), consisting of alternating lamellas of the phases α_2 and γ , is documented in **Fig. 1**.

More detailed view of lamellar grains is shown in **Figs. 2** to **4**. In these figures it can also be seen that both Ta and Nb alloyed alloys, in addition to already mentioned lamellar areas, contain also minor proportion of β phase and interdendritic γ -phase. Yttrium alloyed alloys contain moreover yttrium-rich phases. It was established by detailed observation of the microstructure that the yttrium-rich phases appear in the alloy in two different forms. The first one showed larger size (up to 30 μm) and it was identified by EDS analysis of chemical composition analysis as YAl_2 , since the ratio between Y and Al is approximately 1:2, and the determined content of other elements was possibly caused by environmental influences. The second phase showed smaller size, usually ellipsoidal shape and it contained significant content of oxygen. On the basis of the ratio of individual elements it was identified as Y_2O_3 . Presence of these yttrium-rich phases in yttrium alloyed γ -TiAl alloys has also been described in publications [10, 11]. Chemical composition of individual structural areas, including the standard deviations of measurements, is given in **Tables 3** and **4**.

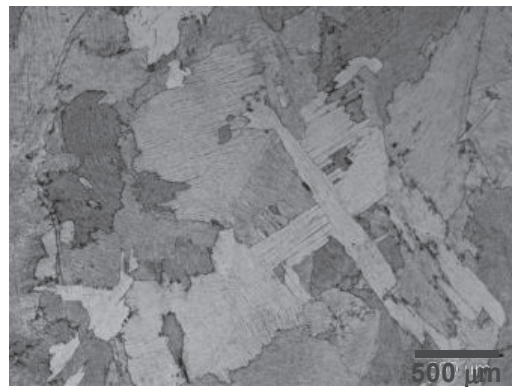


Fig. 1 Microstructure of 8Nb-plasma alloy (OM)

Table 3 Chemical composition of individual phases in samples 8Nb-plasma and 8Nb-Y-plasma (at.%)

| area | Ti | Nb | Al | Y | O |
|------------------------|------------------|------------------|------------------|------------------|------------------|
| β | 47.29 \pm 2.23 | 10.91 \pm 1.26 | 41.80 \pm 1.83 | - | - |
| $\alpha_2 + \gamma$ | 43.15 \pm 0.43 | 8.57 \pm 0.73 | 48.28 \pm 0.53 | - | - |
| γ | 42.27 \pm 2.59 | 6.26 \pm 1.31 | 51.48 \pm 3.64 | - | - |
| YAl_2 | 17.89 \pm 7.47 | 1.45 \pm 1.45 | 57.94 \pm 2.44 | 22.71 \pm 6.56 | - |
| Y_2O_3 | 3.28 \pm 3.41 | - | 5.07 \pm 4.60 | 36.78 \pm 4.33 | 54.87 \pm 3.97 |

Table 4 Chemical composition of individual phases in samples 8Ta-Scast and 8Ta-Y-Scast (at.%)

| area | Ti | Ta | Al | Y | O |
|------------------------|----------------|----------------|-----------------|----------------|----------------|
| β | 42.6 \pm 0.6 | 14.6 \pm 0.9 | 42.8 \pm 0.38 | - | - |
| $\alpha_2 + \gamma$ | 42.8 \pm 1.4 | 9.2 \pm 0.2 | 48.0 \pm 1.3 | - | - |
| γ | 40.7 \pm 2.6 | 2.8 \pm 0.9 | 56.5 \pm 3.5 | - | - |
| YAl_2 | 20.5 \pm 4.6 | 1.1 \pm 1.1 | 58.5 \pm 2.8 | 19.9 \pm 6.5 | - |
| Y_2O_3 | 15.5 \pm 2.5 | 1.0 \pm 1.0 | 22.1 \pm 3.6 | 21.3 \pm 2.8 | 40.1 \pm 3.4 |

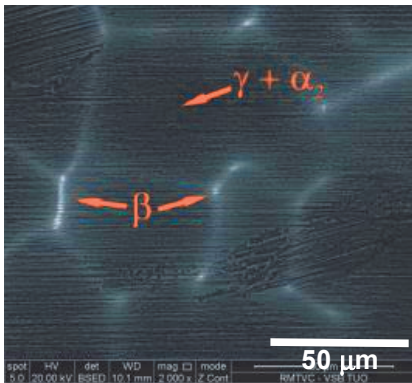


Fig. 2 BSE image of the 8Nb - plasma sample

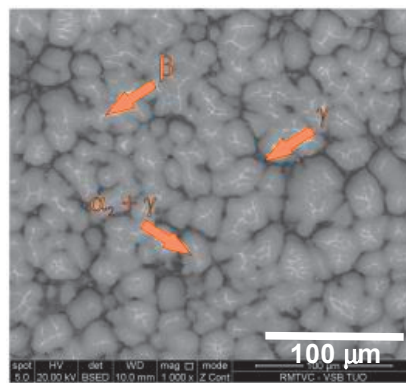


Fig. 3 BSE image of the 8Ta-Y - Scast sample

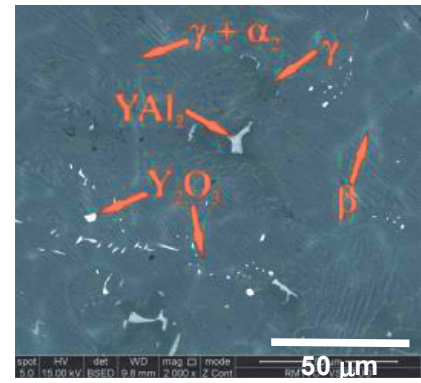


Fig. 4 BSE image of 8Nb-Y - plasma sample

3.2. Microstructure of alloys after heat treatment

Micrographs of the microstructure of samples after annealing are shown in **Figs. 5** and **6**. As it can be seen in these photos, the microstructure contained comparatively high share of fine γ_m grains (70-80% in the alloys alloyed with Nb and 50-70 % in alloys alloyed with Ta), the size of which usually did not exceed 50 μm . These fine grains were formed from the α phase by massive transformation to the γ_m phase performed by rapid cooling from the temperature characteristic for α area of the Ti-Al binary diagram. With the exception of the γ_m phase, all the samples contained, however, also a minor share (20-30 %) of coarse lamellar grains (L), which usually did not reach a size larger than 100 μm . This means that the massive transformation under the given conditions did not run completely and grains with lamellar structure were formed from non transformed α regions. The alloyed alloys then contained, apart from the aforementioned phase, also relatively high share of non transformed inter-dendritic γ phase (15-30 %). Annealing also caused dissolution of the complete β phase, which was confirmed by observation by electron microscopy.



Fig. 5 Microstructure of the 8Nb-plasma sample after the dissolving annealing (OM)

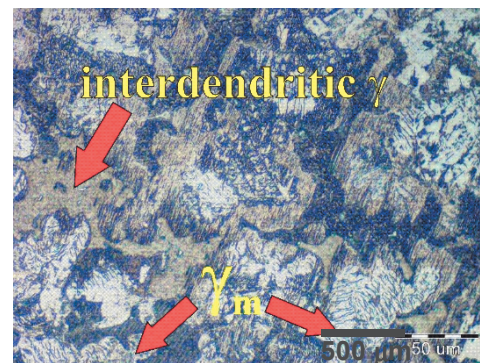


Fig. 6 Microstructure of the 8Ta-Scast sample after the dissolving annealing (OM)

Figs. 7 and **8** show typical microstructure of the samples after subsequent annealing which is carried for the purpose of achieving the convoluted microstructure. As it can be seen in these figures, the above mentioned heat treatment had a very significant effect on the microstructure. The microstructure after annealing of the samples consists of grains of much smaller size than in the as cast state, formed mainly by the massive γ_m phase, in which precipitation of lamellas of the α_2 phase took place during subsequent annealing.

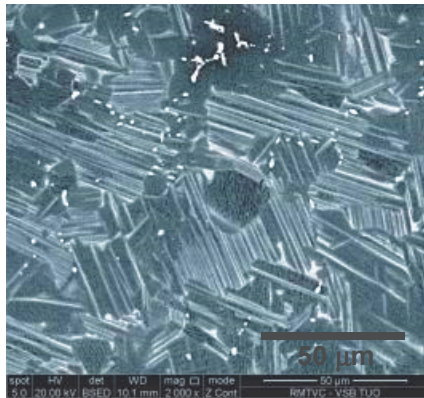


Fig. 7 Microstructure of the 8Nb-Y-plasma sample after the ageing

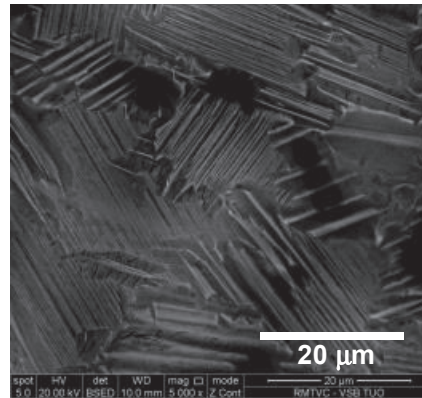


Fig. 8 Microstructure of the 8Ta-Scast sample after the ageing

The results of EDS analyses of chemical composition of the phases of both samples are presented in **Table 5**. The alloys alloyed with yttrium contain moreover yttrium-rich phases YAl_2 and Y_2O_3 . Almost no differences were observed in distribution, size and chemical composition of the yttrium-rich phases in comparison with the samples before heat treatment. The average grain size in all the samples in the as-cast state and after heat treatments, determined by linear method, is presented in **Table 6**. The alloy alloyed with yttrium thus exhibits in both cases slightly smaller average grain size, however, the detected difference is not too distinct.

Table 5 Results of EDS analysis of the phase composition in samples after heat treatment (at.%)

| 8Nb-plasma | Ti | Nb | Al |
|-------------------------|--------------|--------------|--------------|
| α_2 | 47.87 ± 0.14 | 8.16 ± 0.09 | 43.97 ± 0.22 |
| γ | 41.31 ± 0.29 | 7.02 ± 0.33 | 51.67 ± 0.10 |
| 8Nb-Y-plasma | Ti | Nb | Al |
| α_2 | 48.59 ± 0.44 | 9.03 ± 0.94 | 42.38 ± 1.14 |
| γ | 41.30 ± 0.37 | 7.71 ± 0.39 | 50.99 ± 0.48 |
| 8Ta-Scast | Ti | Ta | Al |
| α_2 | 45.00 ± 0.32 | 10.42 ± 0.21 | 44.58 ± 0.35 |
| γ | 42.51 ± 0.04 | 8.78 ± 0.44 | 48.71 ± 0.44 |
| interdendritic γ | 42.79 ± 0.50 | 5.31 ± 0.66 | 51.9 ± 0.21 |
| 8Ta-Y-Scast | Ti | Ta | Al |
| α_2 | 46.07 ± 1.28 | 9.58 ± 0.65 | 44.35 ± 0.76 |
| γ | 42.66 ± 0.10 | 7.72 ± 0.31 | 49.62 ± 0.32 |
| interdendritic γ | 43.03 ± 0.18 | 5.24 ± 0.30 | 51.73 ± 4.24 |

Table 6 Mean grain size of the samples in the as-cast state and after heat treatment

| Sample | Grain size (µm) | |
|--------------|-----------------|---------------|
| | As-cast state | After HT |
| 8Nb-plasma | 339.66 ± 100.66 | 68.56 ± 22.61 |
| 8Nb-Y-plasma | 330.91 ± 131.11 | 51.47 ± 24.54 |
| 8Ta-Scast | 230.47 ± 61.01 | 36.83 ± 15.86 |
| 8Ta-Y-Scast | 203.03 ± 33.75 | 35.31 ± 7.36 |

3.3. Mechanical properties in compression at room temperature

The average values of proof stress, yield strength, tensile strength and plastic deformation determined during compression tests of heat-treated samples are presented in **Table 7**. As it can be seen from this comparison, the heat treatment had a very significant effect on mechanical properties in compression. It is evident already at the first glance that the heat treated samples exhibited much more distinct yield stress, much higher values of deformation and also higher strength. Average values of proof stress in all alloys after heat treatment was reduced at room temperature, namely from 750 MPa for the alloy 8NB-plasma to 464 MPa, and from 1023 MPa for the alloy 8NB-Y-plasma to 549 MPa.

Table 7 Comparison of mean values of mechanical properties of the as-cast and heat-treated alloys in compression at the room temperature

| As-cast state | | | | After HT | | | |
|---------------|------------------|-------------|------------------------|--------------|------------------|-------------|------------------------|
| Sample | $R_{p0.2}$ (MPa) | R_m (MPa) | ε_{Rm} (%) | Sample | $R_{p0.2}$ (MPa) | R_m (MPa) | ε_{Rm} (%) |
| 8Nb-plasma | 750 | 1369 | 10.46 | 8Nb-plasma | 464 | 1925 | 29.83 |
| 8Nb-Y-plasma | 1023 | 1592 | 9.1 | 8Nb-Y-plasma | 549 | 1835 | 24.87 |
| 8Ta-Scast | 795 | 1537 | 15.13 | 8Ta-Scast | 463 | 1744 | 30.21 |
| 8Ta-Y-Scast | 922 | 1791 | 17.3 | 8Ta-Y-Scast | 505 | 1564 | 21.22 |

Similar results were achieved also in alloys alloyed with Ta, which showed a decrease of the average yield strength from 795 MPa to 463 MPa for the sample 8Ta-Scast, and from 922 MPa to 505 MPa for the sample 8Ta-Y-Scast. Significant changes, however, occurred mainly in the values of plastic deformation to R_m . For example in case of the alloy 8 Nb the average value ε_{Rm} after heat treatment was 29.83%, which is much higher than 10.46 % (the value obtained for the same alloy in the as-cast state). Other heat-treated alloy also exhibited similar increase in plastic strain. A significant increase in comparison to the as-cast state was observed also for the ultimate strength values, namely from 1369 MPa to 1925 MPa for the alloy 8NB-plasma, and from 1592 MPa to 1835 MPa for the alloy 8NB-Y. However, in the alloys alloyed with Ta the ultimate strength increased only in the sample-8TA-Scast, namely from 1537 MPa to 1744 MPa, while for the alloy-Y-8TA-Scast, the ultimate strength decreased from 1791 MPa in the as cast state to 1564 MPa in the state after heat treatment.

4. CONCLUSIONS

It was found that solution annealing for a period 10 minutes and followed by cooling in oil for Nb-alloyed alloys and by subsequent cooling by fan caused in Ta-alloyed alloys formation of massive γ_m phase. In addition to massive γ_m phase all the samples contained also a smaller share of non transformed coarse lamellar grains, and Ta-alloyed alloys contained moreover non-transformed inter-dendritic γ phase. No significant changes associated with the addition of 0.3 at.% Y and with different contents of oxygen in the course of massive transformation. Next annealing of the samples resulted in formation of convoluted microstructure by precipitation of lamellar phase α_2 . The value of plastic deformation to R_m in all the samples did not fell below 20 % after heat treatment, which indicates lower brittleness and higher toughness of these materials. Results of mechanical testing in compression thus confirmed the suitability of grain refinement by massive transformation in these alloys, although massive transformation did not run completely in the whole volume of the samples.

ACKNOWLEDGEMENTS

This paper was created in the project No.LO1203 "Regional Materials Science and Technology Centre - Feasibility Program" funded by Ministry of Education, Youth and Sports.

REFERENCES

- [1] LORIA, E.A. Gamma titanium aluminides as perspective structural materials. *Intermetallics*, Vol. 8, No. 9-11, 2000, pp. 1339-1345.
- [2] WU, X. Review of alloy and process development of TiAl alloys. *Intermetallics*, Vol. 14, No. 10-11, 2006, pp. 1114-1122.
- [3] LAPIN, J. TiAl-based alloys: Present status and future perspectives. In: *Metal 2009: 18th International Conference on Metallurgy and Materials*. Ostrava: TANGER, 2009, pp. 1-12.
- [4] SAAGE, H., HUANG, A.J., HU, D., LORETTO, M.H., WU, X. Microstructures and tensile properties of massively transformed and aged Ti46Al8Nb and Ti46Al8Ta alloys. *Intermetallics*, Vol. 17, No. 1-2, 2009, pp. 32-38.
- [5] JIANG, H., ZHANG, K., HAO, X.J., SAAGE, H., WAIN, N., HU, D., LORETTO, M.H., WU, X. Nucleation of massive gamma during air cooling of Ti46Al8Ta. *Intermetallics*, Vol. 18, No. 5, 2010, pp. 938-944.
- [6] HECHT, U., WITUSIEWICZ, V., DREVERMANN, A., ZOLLINGER, J. Grain refinement by low boron additions in niobium-rich TiAl-based alloys. *Intermetallics*, Vol. 16, 2008, pp. 969-978.
- [7] HUANG, A., LORETTO, M.H., HU, D., LIU, K., WU, X. The role of oxygen and cooling rate on transformations in TiAl-based alloys. *Intermetallics*, Vol. 14, No. 7, 2006, pp. 838-847.
- [8] JUŘICA, J., ČEGAN, T., SKOTNICOVÁ, K., PETLÁK, D., SMETANA, B., MATĚJKA, V. Preparation and properties of master alloys Nb-Al and Ta-Al for melting and casting of gamma-TiAl intermetallics. *Materiali in Tehnologie/Materials and Technology*, Vol. 49, No. 1, 2015, pp. 27-30.
- [9] ČEGAN, T., SZURMAN, I., KURSA, M., HOLEŠINSKY, J., VONTOROVÁ, J. Preparation of TiAl-based alloys by induction melting in graphite crucibles. *Kovove mater.*, Vol. 53, No. 2, 2015, pp. 69-78.
- [10] ČEGAN, T., KURSA, M., KONEČNÁ, K., SMETANA, B., ZLÁ, S., MATĚJKA, V., ŽALUDOVÁ, M. Effect of yttrium on oxygen content and microstructure of TiAl intermetallics. In *METAL 2012, 21th International Conference on Metallurgy and Materials*. Ostrava: TANGER, 2012, pp. 1430-1436.
- [11] LI, B., KONG, F., CHEN, Y. Effect of yttrium addition on microstructures and room temperature tensile properties of Ti-47Al alloy. *Journal of Rare Earths*, Vol. 24, 2006, pp. 352-356.